

A new PRBA-based instrument to measure the shape of the cornea

F.M. Vos^{1,2}, G.L. van der Heijde², H.J.W. Spoelder¹, I.H.M van Stokkum¹, F.C.A. Groen³

¹ Faculty of Physics and Astronomy of the Vrije Universiteit,
De Boelelaan 1081, 1081 HV Amsterdam,
tel. +31 20 44 47870, fax +31 20 44 47899, E-mail: vosf@nat.vu.nl

² Faculty of Medicine of the Vrije Universiteit
p.o. Box 7057, 1007 MB Amsterdam,
tel. +31 20 44 40286, fax +31 20 44 44147

³ Faculty of Mathematics, Computer Science, Physics and Astronomy of the University of Amsterdam
Kruislaan 403, 1098 SJ Amsterdam,
tel. +31 20 525 7463, fax +31 20 525 7490

Abstract - We have developed a prototype-instrument providing a new way to measure the shape of the cornea. Our approach exploits properties of Pseudo Random Binary Arrays (PRBA's). Encoded in a coloured pattern (stimulus) that is mirrored to the eye PRBA's allow for unique characterization of positions both in the stimulus and the reflected image. This is used to come to an integral reconstruction of the cornea. It is demonstrated that the new technique contributes to a very robust measurementmethod.

I. INTRODUCTION

The anterior surface of the human eye (cornea) is for 84% responsible for the refraction of light and thus of eminent importance for good sight. Ophthalmologists have recognized the role of the cornea in the refraction process. A modern technique to improve a patient's sight is by adjusting the corneal surface. The rapid development of this keratorefractive surgery induced the need for accurate methods to evaluate the shape of the cornea.

To measure the shape of the cornea standardly a cylindrically symmetrical ringpattern (stimulus) is mirrored to the eye. Analysis of the recorded reflection (Purkinje image) allows for reconstruction of the corneal surface.

Available instruments employing this technique are known not to work ideally [1]. In pathological cases with severely irregular or badly reflecting corneas, automatic recognition of the ringpattern often fails as the mires become extremely distorted or vague. Moreover, as it is impossible to uniquely identify positions along each ring

it has to be assumed that reflection occurs in meridional planes to come to a description of the corneal shape per meridian only.

We have developed a prototype-stimulus that exploits the virtues of Pseudo Random Binary Arrays (PRBA's), which, encoded in a coloured stimuluspattern, contribute to a very robust measurementtechnique with uniquely characterized points. In our approach it is not necessary to make the aforementioned reflection-assumption enabling an integral reconstruction of the cornea.

Details of our design are worked out in Section II. In Section III some experimental aspects of the stimulus are presented and the accuracy and robustness of our approach is studied. Section IV describes the reconstruction of the corneal surface.

II. METHOD

The essence of our novel technique lies in the use of uniquely characterized positions both on the stimulus and in the recorded reflection. In this way a one-to-one correspondence between points on the stimulus and on the registering device is established which can be used to reconstruct the corneal shape. Implementation of this design is facilitated by properties of Pseudo Random Binary Arrays.

Pseudo Random Binary Arrays (PRBA's) ($A[i,j] \mid i < n, j < m, A[i,j] \in \{0,1\}$) are the two dimensional analogon of Pseudo Random Binary Sequences ($S[i] \mid i < n$). Primitive polynomials with coefficients 0 or 1 provide the feedback path of shif-tregisters that are used to generate these maximum length sequences. PRBA's exist in various sizes and have many useful distinguishing features.

The key virtue we use is the “window”-property: each bit-pattern seen through a prescribed window of k -by- l (or larger) bits sliding over the array is unique. Conversely, each k -by- l (or larger) subpart of the PRBA uniquely defines a position in the PRBA. Fig. 1 shows an example of a PRBA (with $n = 3$, $m = 5$, $k = 2$, $l = 2$). For a more formal treatment of PRBA's we refer to [2].

We have opted to encode a large PRBA ($n = 65$, $m = 63$, $k = 6$, $l = 2$) through a representation of the 0's and the 1's by two bright colours. A third colour (black in our approach) is necessary to provide distinction between adjacent bits of the same value. The assembled pattern presents a checkerboard pattern when mirrored to a sphere of radius 8 mm (average radius of the human eye). Fig. 2 demonstrates our encoding of the PRBA of Fig. 1 (the 0's and 1's are added for clarity). Each position where two black squares meet (“crossing”) can be uniquely labelled with the positional indices of the adjacent bits in the encoded PRBA.

The prototype-instrument devised by us is depicted in Fig. 3. It consists of a cylinder closed at one side con-

0	1	1	1
0	0	1	1
0	1	0	0

Fig. 1. Example of a PRBA: each subarray of 2 by 2 or larger contains a unique bitpattern.

taining a pattern (stimulus or stimulator) that is brightly lit from the back. The object to be measured is positioned in front of the open end; the reflected image (Purkinje image) is registered with a camera behind the other (closed) end. The camera used in this configuration is a Panasonic 3-CCD camera (GP-US502). Digitization of the resulting image is done with the Matrox Meteor/rgb-framegrabber placed in a Dell Pentium 90 PC. Further processing of the captured information is done on a SUN SPARCclassic workstation within the SCIL-image image-processing environment [5] and the S-plus modelling environment [6].

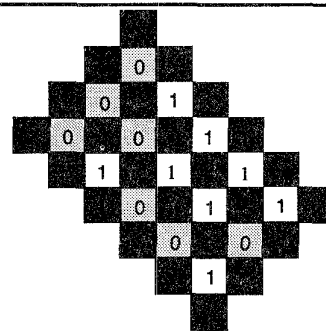


Fig. 2. Example of our encoding: two colours are used to represent the bits of the PRBA of Fig. 1 (the 0's and 1's are added for clarity).

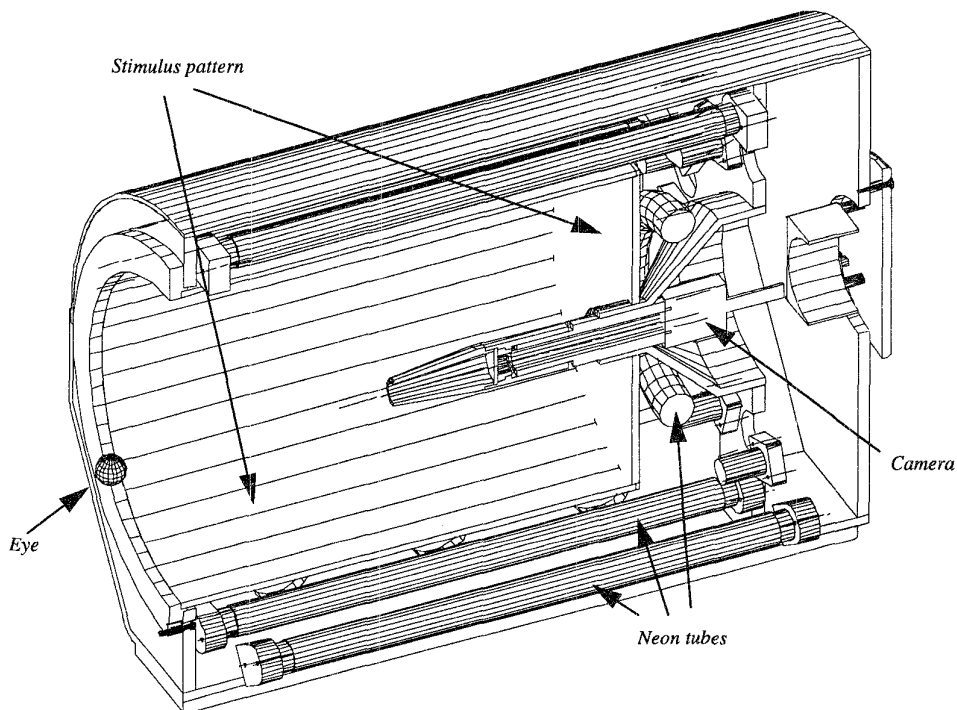


Fig. 3. Crosscut of our prototype. The stimulus pattern, lit from the back by neon tubes, is mirrored to the eye, its reflection is registered with a camera.

III. PATTERN RECOGNITION

A. Implementation

In uniquely identifying the crossings the first step is to localize them in the input image. This is done with a matched filter approach [3]. Locations are accepted as crossings if the response to the matched filter exceeds a preset threshold value. By adjusting the threshold false-positive responses are eliminated. Secondly the colours of the adjacent coloured squares must be determined. In order to do this the relative RGB-values of the pixels of the coloured squares are aggregated, leaving out the pixels of the outermost two layers to diminish the effect of blurring. The relative colour of a pixel (r_i, g_i, b_i) is defined as $(r_i/s_i, g_i/s_i, b_i/s_i)$ where $s_i = r_i + g_i + b_i$. After this the relative colours are clustered with the K-means clustering algorithm into two groups representing the 0's and 1's [4]. If the average relative colour of a square is closer to the centre of the 0-cluster than to the other it is identified as a 0, otherwise as 1. Thus we come to a tentative assignment of bitvalues.

Subsequently, a graph is constituted by linking crossings to their respective neighbouring crossings. Here we take into account that with two neighbouring crossings the configuration of the coloured squares inverts. This process can be conceived as reconstructing the checkerboard pattern. From the checkerboard a binary "sub"-array is recovered (possibly not the entire PRBA is "recognized" as not all the crossings might be identified). Matching of the subarray against the "mother"-PRBA leads to a unique identification of the crossings.

B. Colour experiments

A key problem that had to be solved was which colours should be used in our encoding. Obviously those colours should be taken that provide optimal recognition, also under noisy circumstances. To determine this we mirrored patches of 6 colours (Red, Green, Blue, Cyan, Magenta, Yellow) to a blue eye and a metal ball (as an ideal testobject for comparison), and determined the average relative colour of the reflections registered by our camera.

Fig. 4 (metal ball), Fig. 5 (blue eye) and Fig. 6 (brown eye) show the results projected on the plane $r + g + b = 1$: circles of radius twice the corresponding standard deviation are drawn round each average; along the vertical axis is the normalized blue-coordinate, along the horizontal axis (the sloping lines in the graph) the normalized green-coordinate.

From these figures it can be concluded that red and magenta are indistinguishable. Furthermore, red/magenta, blue and green closely resemble a grey tint (the centre of the graph). Yellow and cyan lie farthest apart, providing the best distinction and thus the most

optimal choice for our encoding.

C. Precision in the localization of pattern elements

The precision of our matched filter approach as to the localization of the crossings was tested in the following experiment.

Artificial images were generated holding a checkerboard of 11 by 11 squares presenting our design. In each simu-

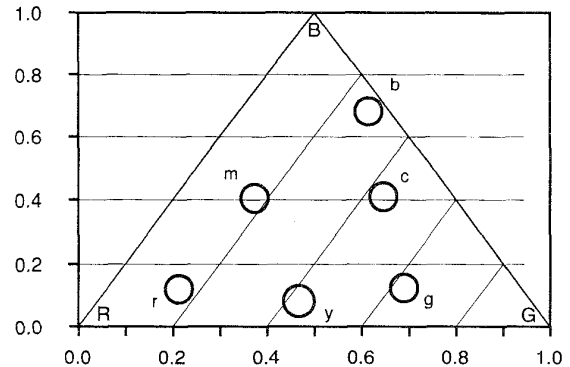


Fig. 4. Relative response of our camera to six coloured patches mirrored to a metal ball: circles of radius twice the standard deviation are drawn round each average (r=Red, m = Magenta, b = Blue, c = Cyan, g = Green, y = Yellow).

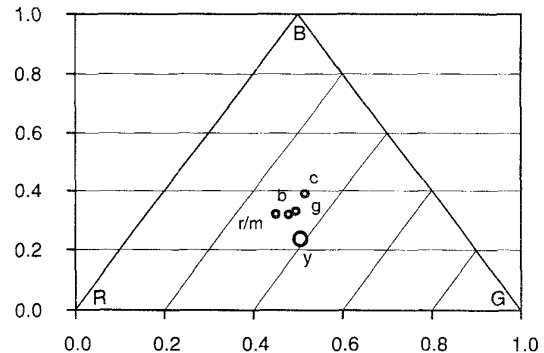


Fig. 5. Relative response of our camera to six coloured patches mirrored to a blue eye

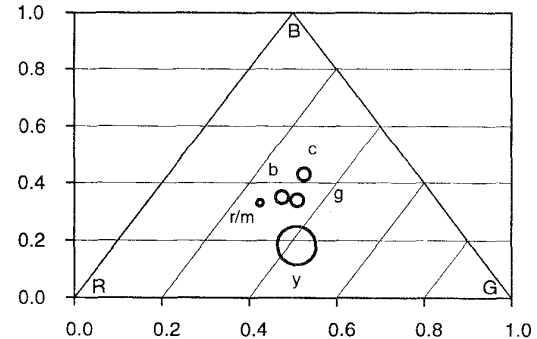


Fig. 6. Relative response of our camera to patches of six colours mirrored to a brown eye

lated image the location of the crossings (100 in total) was exactly known. The distance between neighbouring crossings was set to a prefixed number of pixels (blocksize). The RGB-colour of the black, cyan and yellow squares were taken as (0,0,0), (0,255,255), (255,255,0) respectively. To introduce disturbance uncorrelated uniformly distributed noise of preset standard deviation was added to the individual colour channels separately. In this we try to relate the average distance between the real and detected location (and corresponding standard deviation) to the blocksize and the standard deviation of the applied noise. We expected to find deterioration of the results with small blocksizes and large amounts of noise. Results are collated in Table I.

TABLE I
PRECISION OF OUR LOCALIZATION PROCEDURE: EACH ENTRY PRESENTS THE AVERAGE DISTANCE BETWEEN THE REAL AND DETECTED LOCATION IN PATTERNS WITH DIFFERENT BLOCKSIZES (IN PIXELS) AND WITH DIFFERENT AMOUNTS OF NOISE

Blocksize	Standard deviation of added noise			
	0	50	100	200
14	1.0 (0.5)	1.1 (0.7)	1.1 (0.7)	1.1 (0.7)
12	1.0 (0.5)	1.0 (0.6)	1.1 (0.6)	1.4 (0.7)
10	1.0 (0.5)	1.0 (0.6)	1.0 (0.6)	1.2 (0.7)
8	1.0 (0.5)	1.1 (0.5)	1.0 (0.5)	1.2 (0.6)
6	1.0 (0.5)	1.0 (0.4)	1.0 (0.5)	1.4 (1.0)

The results remain fairly stable under various amounts of noise and with different blocksizes. The procedure fails only with huge amounts of noise (SD 200) and with small blocksize (6 pixels) as the average distance plus twice the standard deviation exceeds half the blocksize. A precision of about 1 pixel in the localization of pattern elements is demonstrated under very noisy circumstances (SD 100) and with small pattern elements (6).

D. Accuracy in the identification of pattern elements

To determine the accuracy of our identification procedure we devised four stimulus patterns containing our encoding. The average blocksize registered by our camera when mirroring these stimuli to a sphere of 8 mm radius was 7 by 7, 9 by 9, 11 by 11 or 13 by 13 pixels. Table II relates the blocksize to the percentage erroneously identified blocks when mirrored to a blue or a brown eye or to a metal ball.

TABLE II
ACCURACY OF OUR IDENTIFICATION PROCEDURE: THE PERCENTAGE OF WRONGLY CLASSIFIED COLOURED SQUARES AT A GIVEN BLOCKSIZE

blue eye		brown eye		metal ball	
average blocksize (pixels)	error %	average blocksize (pixels)	error %	average blocksize (pixels)	error %
6.9	19.2	7.3	21.7	7.0	6.0
9.2	12.1	9.4	16.7	8.9	1.7
11.3	7.5	12.2	16.3	11.2	1.7
13.7	8.6	14.6	11.7	13.1	0.0

The average blocksizes deviate from the blocksizes mentioned previously as the two eyes and the metal ball do not present perfect spheres with 8 mm radius.

From these tables it can be concluded that in the process of recovering the pattern from the input image a significant number of bits will be wrongly interpreted. Thus it is necessary to evaluate to what extent (despite misinterpretations) it is still possible to come to a unique identification of the subpattern (and thus to come to a complete fault correction).

E. Relocation experiments

To investigate the robustness of the PRBA property of unique characterization of subarrays we conducted the following experiment.

From the "master"-PRBA (the one which was used during the course of our project with $n = 63$, $m = 65$, $k = 6$, $l = 2$) all rectangular subarrays were taken of all sizes larger than 6 by 2. In each individual subarray bits were inverted with an a priori taken probability (noise level). Subsequently the master PRBA (M) was searched for the original position of each subarray (S) by sliding the subarray over the PRBA (relocation). At each position (x,y) the Hamming distance was recorded (the number of different bitvalues):

$$H = \sum_{i=1}^k \sum_{j=1}^l |S(i, j) - M(x+i, y+j)| \quad (1)$$

(with k and l the height and the width of the subarray). Correct relocation was admitted if a subarray had an absolute minimum in Hamming distance at its original position. Fig. 7 illustrates this process for a specific subarray containing 1550 bits at noise level 17.5%.

Fig. 8 summarizes the results of the simulations. Along the horizontal axis is the size of the subarray (height times width), vertically the fraction of subarrays of a given size that could be correctly relocated. Each curve corresponds to a different noise level. From this figure it

can be concluded that when no noise is applied all subarrays of all sizes will be correctly relocated. Conversely, the original position of not even one subarray is correctly identified when approximately 50% of the bits are inverted. At a noise level of 20% (worst case in our application, see Table II) a rectangular subarray has to include minimally 150 bits to allow for correct relocation. Experiments with different randomseeds showed identical profiles.

F. Summary of the identification process

From our colourdiagrams it can be deduced that cyan and yellow, located farthest apart, provide the best pick for our encoding. Introduction of more colours (for example to incorporate additional information) is unrealistic as alternatives appear closely to either cyan or yellow (Fig.

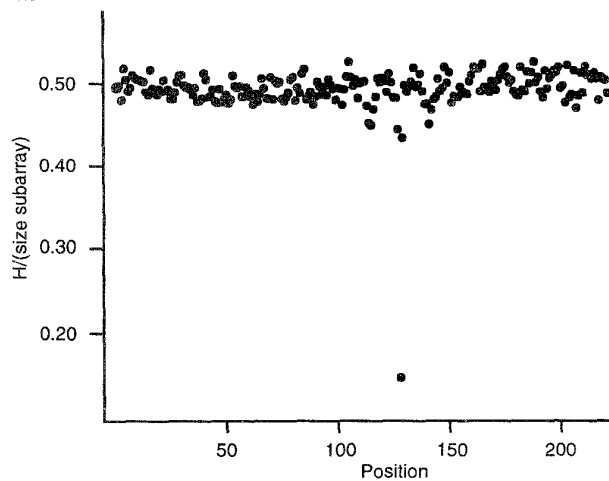


Fig. 7. Normalized Hamming-distance for all possible relocations of a 1550 bit subarray with 17.5% noise; the average normalized Hamming distance is 0.5, at the position standing out it is 0.175.

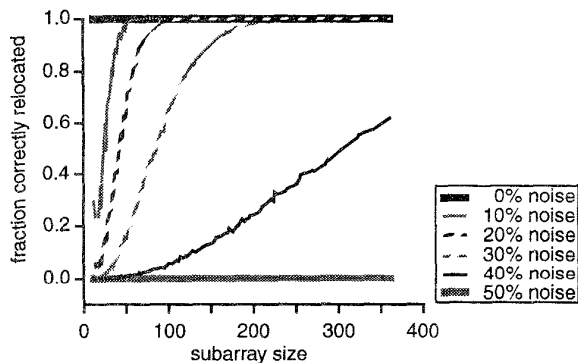


Fig. 8. Relocation properties of a PRBA: a searchprocess was undertaken to the original position of all subarrays of all sizes (relocation). Each curve shows the fraction correctly relocated subarrays of a given size at a specific noise level.

5 and Fig. 6).

Under controlled, simulated circumstances we demonstrated a precision of one pixel in the *localization* of pattern elements, even under noisy circumstances ($10^{10} \log(\text{Signal/Noise}) = 10^{10} \log(255/100) = 4.06$) and with small pattern elements (six by six pixels per element).

When the average size of pattern elements is 7 by 7 pixels approximately 20% of them is wrongly interpreted. These errors can be totally corrected if the pattern contains a rectangular area of at least 150 bits (See Fig. 8). As our prototype contains 4095 coloured blocks (= 65 times 63 bits) a resolution that is even slightly better than that of commercially available instruments (8 pixels per ring) is feasible.

IV. RECONSTRUCTION

Our approach enables an integral reconstruction of the corneal shape whereas standard techniques lead only to a description of the cornea in crosscuts. To exploit the benefit of our method we implemented a reconstruction-algorithm that, as a first approximation, models the corneal shape as an ellipsoid with a fixed centre and 6 degrees of freedom (representing the length of the three axes and three rotation angles).

Suppose a point \mathbf{s} on the stimulus is reflected by the cornea in a point \mathbf{c} on the CCD-chip (see Fig. 9). Given an instance of our modelfunction T , it is possible to calculate a point \mathbf{s}' on the stimulator that would be registered in \mathbf{c} when mirrored to the surface described by T . (This can be done by simple backwards raytracing.) Our objective is to minimize $\|\mathbf{s}' - \mathbf{s}\|^2$ for the crossings in our checkerboard pattern, coming down to nonlinear parameteresti-

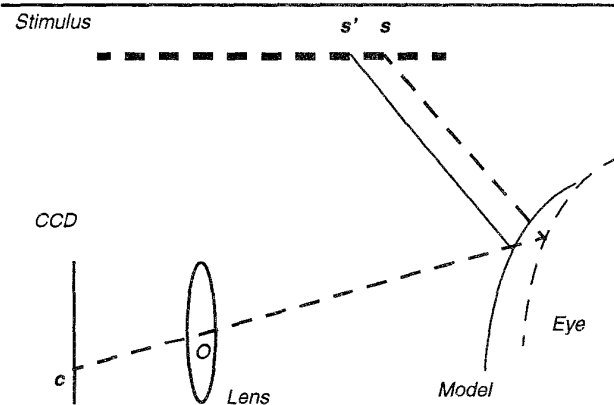


Fig. 9. General outline of the reconstructionprocess: \mathbf{s} is a point on the stimulus that is registered in \mathbf{c} on the CCD; \mathbf{s}' would result in registration in \mathbf{c} when mirrored to an instance of our modelfunction. The distance between all points \mathbf{s} and \mathbf{s}' is minimized by adjusting the parameters of the modelfunction.

mation of the parameters of the model function. For this aim standard parameter estimation procedures are available [6].

We have tested our reconstruction algorithm under artificial circumstances using a raytracing program (POVRAY [7]) as well as with calibrated steel balls and real eyes.

In the raytracing environment a precision of 0.01 mm in the reconstruction of the shape of a sphere of 8 mm was attained.

Table III collates the results of measurements of the radius of three steel balls with our prototype and with a Zeiss keratometer defining the gold standard. Specified are the maximal and minimal radius of curvature in an arbitrary surface point measured with the keratometer. The principal curvatures measured with our instrument are derived from the apex of the reconstructed ellipsoid. The table signifies the close resemblance of the results using fairly ideal test objects.

Table IV holds the curvatures measured of the corneal apex of the right eye of three test persons. It shows that also with nonideal objects the outcome of the two instruments is almost identical.

TABLE III
THE CURVATURE OF THREE STEEL BALLS MEASURED WITH A KERATOMETER AND OUR PROTOTYPE

object	keratometer		cornea-topograph	
	Rmax	Rmin	Rmax	Rmin
1	6.52	6.52	6.49	6.47
2	7.05	7.05	7.01	7.01
3	8.01	8.01	7.99	7.99

TABLE IV
THE CURVATURE OF THE CORNEAL APEX OF THREE EYES MEASURED WITH A KERATOMETER AND OUR PROTOTYPE

subject	keratometer		cornea-topograph	
	Rmax	Rmin	Rmax	Rmin
1	7.94	7.91	7.97	7.88
2	7.80	7.57	7.81	7.68
3	7.36	7.26	7.26	7.23

Thus a precision in the order of that under simulated circumstances is attained, exemplifying the efficacy of our approach.

Currently research is directed towards adjusting the described reconstruction method taking into account local aberrations of the corneal shape as in [8].

V. CONCLUSIONS

Our newly developed instrument exploits properties of Pseudo Random Binary Arrays to capture the corneal surface structure. Encoded in a coloured stimulus pattern PRBA's allow for a unique characterization of positions. Simulations demonstrate a high precision of our procedures in localizing pattern elements. Furthermore, despite a significant number of misinterpretations in the identification of pattern elements, using the characteristics of the encoded PRBA a complete fault correction is demonstrated. As we have introduced a unique characterization of points on the stimulus, integral reconstruction of the corneal shape becomes possible. Thus we have developed a new measurement-technique providing a resolution that is at least as good as that of commercially available instruments.

ACKNOWLEDGMENTS

This research is supported by the Dutch Technology Foundation (STW) under project number VNS33.2983.

REFERENCES

- [1] J.J. Antalis, R.G. Lembach and L.G. Carney, "A Comparison of the TMS-1 and the Corneal Analysis System for the Evaluation of Abnormal Corneas," *the CLAO journal*, vol. 19, pp. 58-63, 1993.
- [2] F.J. MacWilliams and N.J.A. Sloane, "Pseudo-Random Sequences and Arrays," *Proc. of the IEEE*, vol. 64, pp. 1715-1729, 1976.
- [3] P. Vuytsteke and A. Oosterlinck, "Range Image Acquisition with a Single Binary-Encoded Light Pattern," *IEEE Trans. on PAMI*, vol. 12, pp. 148-165, 1990.
- [4] J.A. Hartigan, *Clustering Algorithms*, New York: John Wiley & Sons, 1975.
- [5] R. Van Balen, T. Ten Cate, D. Koelma, B. Mosterd and A.W.M. Smeulders, "Scilimage: A multi-layered environment for use and development of image processing software," in *Experimental Environments for Computer Vision and Image Processing*, H.E. Christensen and J.L. Crowley, Eds. Singapore: World Scientific Press, 1993.
- [6] *S-Plus Programmer's Manual, Version 3.2*, Seattle: StatSci (Mathsoft, Inc.), 1993.
- [7] A. Enzman, L. Kretschmar and C. Young, *Raytracing worlds with POV-Ray*, ISBN: 1-878739-69-7.
- [8] M.A. Halstead, B.A. Barsky, S.A. Klein and R.B. Mandell, "A spline surface algorithm for reconstruction of corneal topography from a videokeratographic reflection pattern," *Optometry and Vision Science*, vol. 72, pp. 821-827, 1995.